Communications of BAO, Vol. 69, Issue 2, 2022, pp. 256-264

# Substructures in the Isolated Galaxy Clusters

E.A. Panko *[1,2], S. Yemelianov[1], A. Sirginava[1], and Z. Pysarevskyi[3]

[1]I.I. Mechnikov Odessa National University, Odessa, Ukraine
[2]Pavol Jozef Safarik University in Kosice, Kosice, Slovak Republic
[3]National Centre "Junior Academy of Sciences"under the auspices of UNESCO, Dnipro, Ukraine

**Abstract**

The isolated clusters are special objects for understanding the ways of forming observed large-scale distributions of matter. One can consider the isolated clusters as objects evolving without any external influence. We present the results of the analysis of the $2D$ distribution of galaxies in 31 isolated galaxy clusters with redshifts $z < 0.15$ and the distance to the nearest neighbor less than $60h^{-1}Mpc$. We defined the morphological types of these clusters accordingly to advance Panko's classification scheme using the "Cluster Cartography" set. The main part of these clusters belongs to the open O-type clusters without any signs of a complex structure. However, we detected the presence of the inner regular substructures for 10 clusters. They are linear substructures, X- and Y-type crosses, and compact short chains. All substructures were detected on a statistically significant level. The detected substructures have special orientations of galaxies, which note to their $3D$ type. Practically all studied galaxy clusters are young.

***Keywords:*** *galaxy clusters: morphology; galaxies: orientation*

## 1. Introduction

The modern approach to the status of galaxy clusters is the idea that these objects are the elements of the Large Scale Structure (LSC) of the Universe and evolve in interaction with other LCS elements. Observed features in the inner structure of galaxy clusters reflect this interaction and arise due to the global influence of the most massive cluster components – dark matter (DM) and intracluster gas. It was studied in different theoretical works from Zeldovich (1970) and Peebles (1969), numerical simulations (Springel et al. (2005), Vogelsberger et al. (2014), Artale et al. (2017), Cui et al. (2018), Tomoaki et al. (2021)) and observed data analysis (Wen et al. (2009), Dietrich et al. (2012), Parekh et al. (2020)). At the same time, the galaxies were and are confident optical markers of the common inner structure of the clusters. It can be noted from the comparison of the distribution of hot gas and galaxies inside the cluster (Tugay et al. (2016)). It has common characteristics: simple distribution of gas observed in $\gamma$- and X-rays corresponds to regular visual morphology of the clusters, or gas disturbed distribution shows the agreement with optically detected cluster substructures, for example, Dietrich et al. (2012). Common characteristics in the DM, hot gas, and galaxies distributions are disturbed in collided clusters Markevitch et al. (2004), where we observe the separation of DM from other cluster components.

The inner structure of galaxy clusters from Abell (1958) and Zwicky et al. (1968) papers is described in the different morphology schemes, based on the positions of the cluster members mainly. The schemes take into account richness, concentration to the cluster's center, and the presence or excess of some special types of galaxies. The Bautz & Morgan scheme (Bautz & Morgan, 1970, BM) is based on the relative contrast (dominance in extent and brightness) of the brightest galaxy to other cluster members. Rood & Sastry (1971) (RS) and later Struble et al. (1987) schemes note the features in the geometry of the distribution of the ten brightest cluster members. Oemler recognized spiral rich and spiral poor galaxy clusters and introduced the special type having giant dominated elliptical cD galaxy in the center. Bahcall (1999) published the common review of morphological schemes. Panko (2013) and AName et al. (2019) based on the different approaches proposed numerical criteria for describing the $2D$ structure of galaxy clusters. This approach also allows detecting the regular linear substructures. Accordingly to Rood & Sastry (1971) and Struble

*panko.elena@onu.edu.ua, panko.elena@gmail.com Corresponding author

et al. (1987) ideas they are the key to the way to the evolution of galaxy clusters: from the open structure without any substructures to the strongly regular concentrated cluster with a giant cD galaxy in the center.

Our study of the detailed morphology of galaxy clusters allowed the detection of some additional kinds of regular substructures, such as crosses, semi-crosses, or curved compact chains (Panko & Emelyanov (2021)). One can assume these substructures as a sign of complex interaction with the underlying DM filaments and the influence of the nearest clusters. One more feature in the detected regular peculiarities is the alignment of galaxies from the brightest and most massive cluster members according to the parent structure to the prevalent orientation of galaxies belonging to the substructure (Panko et al. (2021)). In the second case, we have a the possibility to divide wall-type substructures from filament-type, using the Joachimi et al. (2015) results, even if we have no measured redshifts. Isolated galaxy clusters have influence from the neighbors and we can study the interaction with the underlying LSC elements in pure.

The paper is organized in a standard manner. Section 2 contains the description of the observational data, section 3 explains the cluster mapping and character of substructures, section 4 presents the results and their analysis, and conclusions are given at the end.

## 2. Observational Data

The main base of our study is the list of galaxies obtained from 216 digitized plates of Muenster Red Sky Survey Ungruhe et al. (2003), hereafter MRSS, and based on the MRSS "A Catalogue of Galaxy Clusters and Groups" (Panko & Flin, 2006, PF hereinafter).

The MRSS plates covered about 5000 square degrees of sky with galactic latitudes $b < -45°$. and contained information on more than 5 million galaxies. For each galaxy except for equatorial coordinates and $r_F$ magnitude, a lot of other parameters are given, particularly, the size of axes of the galaxy image in best-fitted ellipse approximation (in *arcsec*), ellipticity, and the position angle of the major axis. The MRSS list contains only galaxies, the stars and perturbed objects were deleted by an automatic procedure with a posterior visual check of the automatic classification, which considerably diminished the number of objects erroneously classified as galaxies. So, MRSS is a statistically valid input list for further research. The $r_F$ magnitudes of galaxies were obtained with external CCD calibration of the photographic magnitudes. There are about 1.2 million galaxies in MRSS completeness limit $r_F = 18.3^m$. This list was used as input data for the creation of the PF catalogue. Each PF cluster has several parameters including Right Ascension and Declination (2000.0), equivalent radius in *arcsec* for the full area of the structure, the number of galaxies, major and minor semiaxes of the best-fitted ellipse, the ellipticity of the structure ($E = 1–b/a$), the position angle of the major axis of structure (counted clockwise from direction to the North Pole, same as the position angle for galaxies in the MRSS), and also the full list of galaxies in the cluster field. Unfortunately, MRSS was the last photographic survey with corresponding weaknesses, and their galaxies have no redshifts.

The comparison of PF catalogue with ACO Abell et al. (1989) and APM Dalton et al. (1997) catalogues allows to estimate the distances to PF galaxy clusters as the $logz$ vs. $m_{10}$ relation Biernacka et al. (2009), following Dalton et al. (1997).

1711 PF galaxy clusters with $z_{est} < 0.15$ and richness over 50 galaxies allowed to create the list of galaxy superclusters Panko (2011) using *FoF* method in Zeldovich & Einasto (1982). Simultaneously, for each of these clusters, the distance to the nearest neighbor was determined. The distribution of distances is shown in Fig. 1. The clusters from the biggest distances (right "tail" noted in Fig. 1 by the ellipse) were selected for the present study as isolated.

The question about the limit distance allowed assuming the cluster as isolated is not obvious. For example, Lee (2012) studied the relative abundance of isolated clusters as a probe of dark energy under the assumption that those galaxy clusters which do not belong to the superclusters are referred to as the isolated. From another hand, one can assume the nonrandom orientation of galaxy clusters is caused due to interaction with neighbors. Firstly this effect was described in Binggeli (1982) paper as the cluster's tendency to be aligned pointing to each other at the separation of up to $15h^1Mpc$. The effect named after Binggeli was observed at various distances and was detected for ranges from $10h^{-1}Mpc$ till $150h^{-1}Mpc$ . It was observed that the strength of the effect diminished with distance (Struble & Peebles (1985), Flin (2019), Ulmer et al. (2019), Biernacka et al. (2015)). It is currently believed that the effect occurs over distances till $60h^{-1}Mpc$ and we selected this value for our study. Moreover, this value is a good criterion for isolated clusters. It is close to another one, which we formally calculated based on the median and standard deviation of the distribution of distances to the nearest neighbor (Fig. 1).

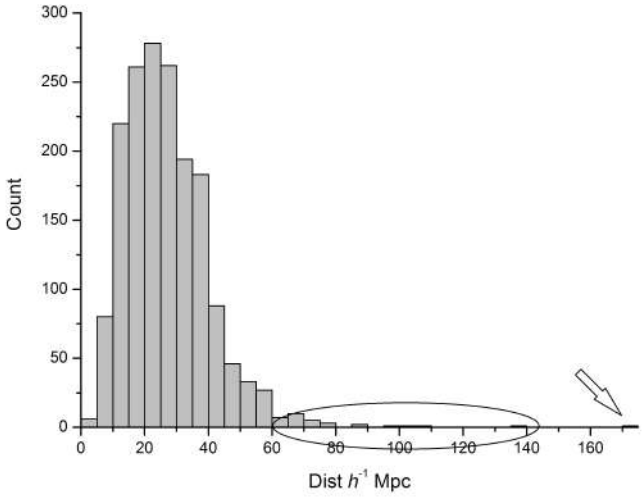


Figure 1. The examples of distribution of the galaxies in the isolated clusters. Right panel to the nearest neighbor for 1711 PF clusters. Isolated clusters are shown by the ellipse. Excluded cluster is marked by the arrow.

We've selected 32 PF galaxy clusters with a richness of 50 and more having neighbors no closer than $60h^{-1}Mpc$, and we checked additionally the presence of the galaxy groups with a richness of less than 50 for selected clusters. We suppose these clusters are placed in relatively low-density environments without any close neighbors. The PF 0540-5764 cluster having the largest distanse ($173.7h^{-1}Mpc$) is located near the boundary of MRSS region and we excluded it from the present study. It is shown in the Fig. 1 by arrow.

Our data set contains 31 PF isolated galaxy clusters with the richness 50 and more galaxies in the cluster field and information about these galaxies. 9 clusters have identifications with ACO, and only 4 with APM catalogues. It can be explained by the lesser depths of the corresponding sky surveys. Only 5 clusters in the data set belong to the rich clusters ($N > 100$), while others contain from 50 to 88 galaxies in the cluster field. The main part of our isolated clusters, 19 ones, have richness from 50 to 60 galaxies, they are poor clusters. 22 isolated clusters have $z_{est}$ in the range 0.10 – 0.14.

## 3. Cluster Mapping and substructures detection

The criteria of the advanced detail morphology scheme were described in Panko (2013) for base regular features in the clusters, such as the degree of concentration to the cluster center or/and to some line. The first character is noted as C, I, or O for clusters with significant, intermediate, or low concentration to the center correspondingly. The linear substructure is noted as L. The role of the brightest galaxies can be marked too. "Cluster Cartography" tool (hereafter CC) was created for cluster mapping and statistical analysis of the distribution of galaxies in the cluster field (Panko & Emelyanov (2015)). The tool allows for creating the 2D cluster map, the symbol for each galaxy corresponds to MRSS data.

The study of the morphology of PF clusters expanded the list of regular substructures (Panko & Emelyanov (2017)), and respectively CC was upgraded (Panko & Emelyanov (2021)). All CC maps have the same size $4000 \times 4000\,arcsec$. The size, shape, and orientation of symbols for galaxies correspond to MRSS data: magnitude $m$, ellipticity $E$, and positional angle of the major axis $PA$ of the galaxy image in the best-fitted ellipse. The size of the symbol $m'$ is calculated from the magnitude as

$$m' = 3 \cdot 2^{0.6(18.5-m)} + 6,$$

And the axes $A$ and $B$ of the ellipse having the same square, as:

$$A = \frac{m'}{\sqrt[4]{(1-2E+E^2)}}, \quad B = \frac{(m')^2}{A}.$$

The legend of the symbol size is shown in $a$ panel in Fig. 2. The typical value for ellipticity 0.2 and positional angle 45° were used for the legend.

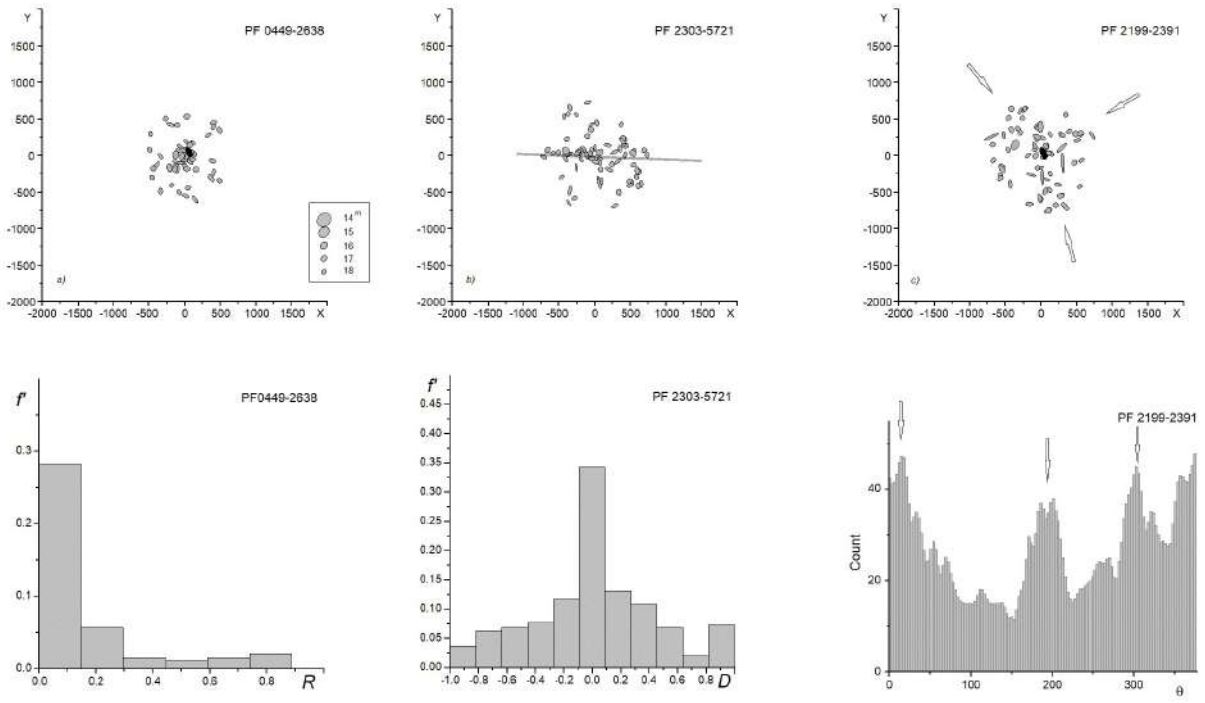


Figure 2. The distribution of galaxies for some isolated clusters: *a)* concentrated cluster, standard case; *b)* linear substructure; and *c)* Y-type substructure. The cluster maps are shown in the upper panel and respective distributions are in the lower one. The brightest galaxy in the C-type cluster is shown as black. The legend of the symbols according to the magnitudes of the galaxies is presented in the *a)* panel.

The numerical analysis of the CC input data is executed automatically and the results can be seen in the Fig. 2. The maps for C-type cluster, OL11- and OY-types are presented in the upper panel as *a*, *b*, and *c*. All clusters are belonged to isolated. The distribution of the density of galaxies is shown in the lower panel for the same map. For PF 0449-2638 the variations of the density along the cluster radius show the significant peak for the central zone. The brightest galaxy of the cluster is shown as black, but the difference between second- and third-ranked galaxies is not significant; it is the brightest cluster member, but not cD galaxy. We attribute this cluster to a typical C-type. Its evolutional status is: greatly evolved. This cluster is not so massive, it is possible cD stage would not be achievable.

The PF 2303-5721 cluster is shown in the *b* map. It has no concentration to the cluster center, it's an open type. The linear substructure is clearly seen in the distributions of densities of galaxies in the stripes. CC automatically detects the direction of the densest stripe. Attribution for PF 2303-5721 is OL11, where 11 is the ratio of the cluster diameter to the width of the overdense stripe. The direction of the linear substructure is shown in the map as the line. The status of the PF 2303-5721: the middle stage of evolution.

The Y-type crumbly substructure in the open cluster is present in *c* part. The crossed substructures can be detected using the "lighthouse beam" diagram. The beam with a width of some part of the diameter (from 1/5 to 1/11), is rotated with step 1°, and the number of galaxies for each position of the beam is shown in the lower part. Three peaks in the distribution correspond to Y-type substructure (pointed by arrows for both panels). PF 2199-2391 cluster we assume as OY type, pertaining to the early stage of evolution.

In this way, the morphological types and presence of features were determined for all 31 isolated clusters.

## 4. The Morphology, Evolutionary Status and Substructures in the Isolated Galaxy Clusters

The morphological classification of 31 isolated PF galaxy clusters is present in Table 1, Appendix A. Only 1 cluster has a significant concentration to the center and can be considered as evolved. 6 clusters have intermediate concentrations with different levels from clearly seen to possible presence. Other clusters are

open, with or without substructures. This common distribution by types corresponds to the assumption that isolated clusters are young structures formed during the general evolution of LCS. The more interesting is the presence of different types of substructures in the isolated clusters. Parts of the filaments with different densities can appear both as elongated clusters and as linear substructures inside a cluster. The interaction of filaments contributes to the appearance of substructures. The rich cluster PF 0413-3091 in which 2 cores are clearly detected, deserves a separate analysis after studying its $3D$ structure when the measured redshifts for its galaxies are obtained.

2 Spiral-rich clusters PF 2188-7165 and PF 2199-2391 are additional evidence of the early stage of cluster evolution. According to the classical work Dressler (1980), spiral (disk) galaxies are destroyed during prolonged interaction with other cluster members. Later papers (Fasano et al. (2000)) note that dependence is ambiguous, and the shapes of galaxies in individual clusters appear to relate to local conditions. X and Y substructures in the PF 2195-7771 and PF 0375-7764 clusters can arise due to crossing the DM underlying filaments. 2 clusters contain special substructures (Fig. 3).

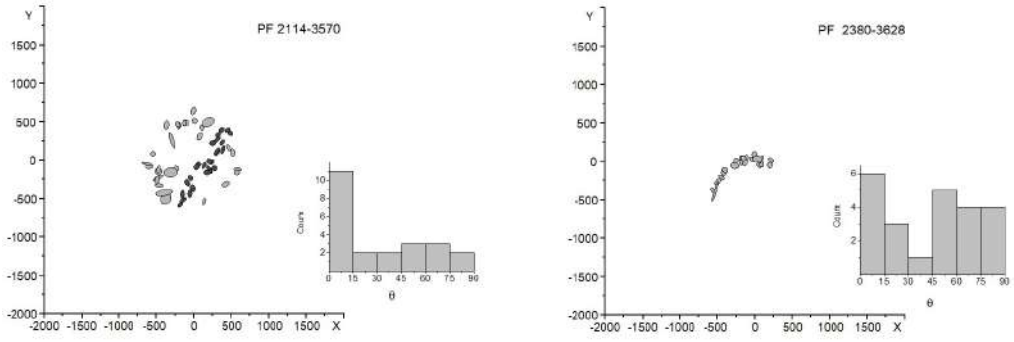


Figure 3. The linear compact chain in PF 2114-3750 (dark symbols), and curved stripe extracted from PF 2380-3628 cluster. The distributions of orientations of the galaxies relative to the common direction of the substructures are shown too in the histograms for both cases.

X and Y substructures in the PF 2195-7771 and PF 0375-7764 clusters can arise due to crossing the DM underlying filaments. 2 clusters containing special substructures are shown in Fig. 3. The compact chain in the PF 2195-7771 contains 23 galaxies that have significant alignment along the parent structure. At less, for galaxies with ellipticity $E > 0.25$ the acute angle between the directions of their major axis and the parent structure less, then 30°. For the curved stripe in PF 0375-7764 we see another distribution. Half of the galaxies in this structure tend to be perpendicular to the central line of the stripe. Both these cases have z good agreement with Joachimi et al. (2015) modeling. In this approach, elliptical galaxies tend to align their major axes with the filament direction, while disc galaxies tend to align their spin perpendicular to the filament direction, and in $2D$ projection we'll see the general alignment of galaxies according to the filament. In another case, in a two-dimensional structure, elliptical galaxies tend to align their major axes along the structure, while disc galaxies tend to align their spin in the perpendicular direction, and we'll not see prevailing orientations. For our data, the substructure in PF 2195-7771 probably is filament-type, while the curved stripe in PF 0375-7764 is the projection of wall.

## 5. Conclusion

We determined the morphological types for 31 isolated PF galaxy clusters according to Panko (2013) scheme. We assumed the isolated clusters are formed in relatively low-dense regions and connected with the underlying DM filaments. They formed later than galaxy clusters in the rich regions. Our results confirm this point of view. The majority of the clusters (25 of the 31) are open clusters, 6 have a different level of concentration to the cluster center, and only 1 is a concentrated one. The direction of the evolution is: from an open cluster without a regular inner structure to a cluster with a well-formed core that contains a giant elliptical cD galaxy. The part of the open clusters for isolated ones is bigger than for the common list. 2 Spiral-rich clusters can be recognized as young too. So, our isolated clusters are newly formed young objects. Our observational data confirmed this position.

For 7 clusters of galaxies, we found regular substructures, namely, linear belts, one compact chain, one curved stripe, and the X- or Y-type substructures, without the correlation between the richness and


doi:https://doi.org/10.52526/25792776-22.69.2-256

substructures' presence. The orientations of galaxies in the detected substructures are in agreement with Joachimi et al. (2015) model and confirm the validation of the substructures.

**Acknowledgements**

This research has (was) made use of (using) NASA's Astrophysics Data System. E. Panko thankful to the SAIA n. o. the National Scholarship Program of the Slovak Republic and Pavol Jozef Safarik University in Kosice for the particular support of this study.

# References

AName A. A., Name B. A., Name A. C., et al. 2019, Proc. Polish Astron. Soc., 2, 85

Abell G. O., 1958, Astrophys. J. Suppl. Ser. , 3, 211

Abell G. O., Corwin H. G., Olowin R., 1989, Astrophys. J. Suppl. Ser. , 70, 1

Artale M. C., Pedrosa S. E., Trayford J., et al. 2017, Mon. Not. R. Astron. Soc. , 470, 1771

Bahcall N. A., 1999, in Formation of Structure in the Universe. Cambridge University Press, p. 135

Bautz L. P., Morgan W. W., 1970, Astrophys. J. , 162, L149

Biernacka M., Flin P. A., Panko E., 2009, Astrophys. J. , 696, 1689

Biernacka M., Panko E., Bajan K., et al. 2015, Astrophys. J. , 813, 20

Binggeli B., 1982, Astron. Astrophys. , 107, 338

Cui W., Knebe A., Yepes G., et al. 2018, Mon. Not. R. Astron. Soc. , 473, 68

Dalton G., Maddox S., Sutherland W., et al. 1997, Mon. Not. R. Astron. Soc. , 289, 263

Dietrich J. P., Werner N., Clowe D., et al. 2012, Nature. , 487, 202

Dressler A., 1980, Astrophys. J. , 236, 351

Fasano G., Poggianti B., Couch W., et al. 2000, Astrophys. J. , 542, 673

Flin P., 2019, Mon. Not. R. Astron. Soc. , 228, 941

Hoyle B., Masters K. L., Nichol, R. C., et al. 2012, Mon. Not. R. Astron. Soc. , 423, 3478

Joachimi B., Cacciato M., Kitching T. D., et al. 2015, Space Sci. Rev. , 193, 1

Lee J., 2012, Astrophys. J. , 752, 40

Markevitch M., Gonzalez A. H., Clowe D., et al. 2004, Astrophys. J. , 606, 819

Panko E., 2011, Balt.˜Astron., 20, 313

Panko E. A., 2013, Odes.˜Astron.˜Publ., 26, 90

Panko E. A., Emelyanov S. I., 2015, Odes.˜Astron.˜Publ., 28, 135

Panko E. A., Emelyanov S. I., 2017, Odes.˜Astron.˜Publ., 30, 121

Panko E. A., Emelyanov S. I., 2021, Odes.˜Astron.˜Publ., 34, 35

Panko E., Flin P., 2006, Journal Astron. Data., 12, 1

Panko E. A., Flin P., 2014, Odes. Astron. Publ., 27, 32

Panko E. A., Yemelianov S. I., Korshunov V. M., et al. 2021, Astr. Rep. , 65, 1002

Parekh V., Lagana T. F., Tho K., et al. 2020, Mon. Not. R. Astron. Soc. , 491, 2605

Peebles P., 1969, Astron. J. , 155, 393

Rood H. J., Sastry G. N., 1971, Publ.˜Astron.˜Soc.˜Pacific, 83, 313

Springel V., White S. D., Jenkins A., et al. 2005, Nature. , 435, 629

Struble M. F., Peebles P. J. E., 1985, Astron. J. , 90, 582

Struble M. F., Rood H. J., Name A. C., et al. 1987, Astrophys. J. Suppl. Ser. , 63, 555

Tomoaki A. A., Francisco P., Klypin A. A., et al. 2021, Mon. Not. R. Astron. Soc. , 506, 4210

Tugay A. T., Dylda S. S., Panko E. A., 2016, Odes.˜Astron.˜Publ., 29, 34

Ulmer M. P., McMillan S. L. W., Kowalski M. P., 2019, Astrophys. J. , 338, 711

Ungruhe R., Seitter W. C., Duerbeck H., 2003, Journal Astron. Data., 9, 1

Vogelsberger M., Genel S., Springel V., et al. 2014, Mon. Not. R. Astron. Soc. , 444, 1518

Wen Z. L., Han J. L., Liu A. C., 2009, Astrophys. J. Suppl. Ser. , 183, 197

Zeldovich Y. B., 1970, Astron. Astrophys. , 5, 84

Zeldovich Y., Einasto J.and Shandarin S., 1982, Nature. , 300, 407

Zwicky F., Herzog E., Wild P., et al. 1961 – 1968, Catalogue of Galaxies and of Clusters of Galaxies. California Institute of Technology, Pasadena

# Appendices

## Appendix A The Morphology Types of 31 Isolated PF Galaxy Clusters

In Appendix A the results of the morphological classification of 31 isolated PF galaxy clusters according to the Panko (. . . ) scheme are present. The consecutive columns of Table 1 contain the following information:

| | |
|---|---|
| PF | the structure identification, based on the first digits of *R.A.* and *Dec.* of the cluster center; |
| *R.A., Dec.* | Right Ascension, in hours, and Declination, in degrees, of the cluster center for 2000.0; |
| *N* | the number of all galaxies in the cluster field; |
| Dist $(h^{-1})Mpc$ | the distance to nearest neighbor |
| $z_{est}$ | the redshift of the cluster, estimated according to Biernacka et al. (2009); |
| Panko Type | the result of the detailed classification by the Panko scheme; |
| note | additional information. |

Table 1. **Morphology of 31 Isolated PF Galaxy Clusters**

| *PF* | *R.A.* | *Dec.* | N | $z_{est}$ | Dist ($h^{-1}$ Mpc) | Panko type | Note |
|---|---|---|---|---|---|---|---|
| 0016-5711 | 0.1670739 | -57.107367 | 88 | 0.053 | 68.9 | IL7 | 1 |
| 0024-2431 | 0.2472369 | -24.300611 | 52 | 0.129 | 78.5 | O | 2 |
| 0093-3597 | 0.9354548 | -35.969931 | 51 | 0.121 | 62.7 | O | |
| 0096-3921 | 0.9621619 | -39.205838 | 52 | 0.142 | 136.9 | O | |
| 0115-4600 | 1.1567254 | -45.996573 | 261 | 0.04 | 105.4 | O | 3 |
| 0145-2632 | 1.4517246 | -26.313951 | 51 | 0.13 | 60.1 | O | |
| 0200-2252 | 2.0036788 | -22.519040 | 52 | 0.133 | 73.0 | O | 4 |
| 0240-4218 | 2.4023855 | -42.175194 | 56 | 0.14 | 98.3 | O | 5 |
| 0294-2398 | 2.9476380 | -23.972509 | 52 | 0.131 | 64.0 | O | |
| 0303-4097 | 3.0337096 | -40.962828 | 53 | 0.127 | 60.5 | O | 6 |
| 0341-3468 | 3.4138816 | -34.671654 | 50 | 0.118 | 60.0 | I | |
| 0358-6952 | 3.5873377 | -69.511811 | 53 | 0.126 | 68.8 | O | |
| 0375-7764 | 3.7591708 | -77.637521 | 54 | 0.126 | 67.4 | OY | |
| 0381-1788 | 3.8163216 | -17.879863 | 282 | 0.069 | 73.5 | O | 7 |
| 0397-6046 | 3.9736611 | -60.450522 | 75 | 0.115 | 71.4 | O | |
| 0413-3091 | 4.1336041 | -30.907580 | 271 | 0.064 | 77.0 | I P | 8 |
| 0444-3673 | 4.4464843 | -36.724158 | 56 | 0.133 | 101.0 | O | |
| 0449-2638 | 4.4987465 | -26.377217 | 54 | 0.124 | 68.9 | C | 9 |
| 0450-6452 | 4.5014199 | -64.516471 | 59 | 0.118 | 71.4 | O | |
| 0501-3610 | 5.0177646 | -36.090484 | 61 | 0.123 | 78.0 | O | |
| 2104-4422 | 21.0417124 | -44.215199 | 56 | 0.123 | 66.8 | O | |
| 2114-3750 | 21.1438407 | -37.493762 | 55 | 0.127 | 69.0 | OL7 cc | 10 |
| 2169-2686 | 21.6904909 | -26.851294 | 57 | 0.130 | 65.4 | O | |
| 2175-1751 | 21.7500206 | -17.503100 | 79 | 0.125 | 87.4 | O | |
| 2188-7165 | 21.8810032 | -71.642227 | 102 | 0.062 | 64.3 | O | 11 |
| 2190-6118 | 21.9097413 | -61.171245 | 58 | 0.119 | 73.1 | O | 12 |
| 2195-7771 | 21.9567135 | -77.709296 | 50 | 0.144 | 89.1 | OX | |
| 2199-2391 | 21.9915162 | -23.900561 | 70 | 0.109 | 62.6 | I L5 | 13 |
| 2204-7192 | 22.0482039 | -71.910053 | 262 | 0.051 | 67.4 | O | |
| 2303-5721 | 23.0319804 | -57.207073 | 70 | 0.119 | 65.4 | IL11 | 14 |
| 2380-3628 | 23.8044115 | -36.274714 | 65 | 0.126 | 69.7 | O cs | 15 |

Types: O – open, I – intermediate, C – compact cluster, according to concentration to the cluster center; L11, etc. — linear substructure; X, Y – X- or Y-type substructure, P – nonstandard feature, cc – compact chain, and cs – curved stripe.


doi:https://doi.org/10.52526/25792776-22.69.2-256

Notes:
[1] PF 0016-5711, identification with ACO 2731
[2] PF 0024-2431, elongated cluster
[3] PF 0115-4600, identification with ACO 2877 and APM 147
[4] PF 0200-2252, identification with ACO S 213
[5] PF 0240-4218, identification with ACO 3014
[6] PF 0303-4097, identification with ACO 3081; negligible concentration to the cluster center, possible classification I?O
[7] PF 0381-1788, identification with ACO 464
[8] PF 0413-3091, double core; identification with ACO 3223 and APM 484
[9] PF 0449-2638, identification with ACO 495 and APM 503
[10] PF 2114-3750, 23 galaxy in the compact chain
[11] PF 2188-7165, Spiral-rich cluster
[12] PF 2190-6118, elongated cluster
[13] PF 2199-2391, 24 galaxy in the compact in the linear substructure, Spiral-rich cluster
[14] PF 2303-5721, possible short chain
[15] PF 2380-3628, curved stripe